Approximate yet essential: advocating for a comprehensive seismic acquisition equation to guide single-sensor adoption

Andrey Bakulin, Bureau of Economic Geology, University of Texas at Austin; Ilya Silvestrov, EXPEC Advanced Research Center, Saudi Aramco*

Summary

Designing better "seismic" is a universal goal. We advocate that it should be done with the ultimate aim of fulfilling what end-users require, casting their requirements as the signal-to-noise ratio of the final image. We demonstrate that a signal-strength model (SSE) captures the main impact of all acquisition parameters, including trace density, array size, and source strength. This is numerically validated using the complex SEAM Arid 3D dataset, with a focus on analyzing single-sensor geometries that can deliver similar or better final image quality than current ones with arrays. We further emphasize the significant role of source strength. This is contrasted with alternative approaches that claim trace density and sampling are key to controlling outcomes, yet fail to offer a comprehensive acquisition equation like the SSE model. In summary, having an approximate acquisition equation is better than having none.

Introduction

Seismic acquisition is constantly evolving, focused on improving products derived from seismic data for various exploration and monitoring purposes (Meunier, 2011; Monk, 2020). Recent advancements in receiver technologies, including nodal receivers and Distributed Acoustic Sensing (DAS), combined with the progress in machine learning for data processing, open up numerous promising geophysical pathways for further advancement. As we progress with the integration of new seismic acquisition technologies, the necessity for a comprehensive approach to evaluate their impact on outcomes becomes evident. It is critical to recognize that the end-users of seismic data, including geologists and interpreters, prioritize the quality of the final image for their geological or engineering projects above our internal advancements. Their primary concern lies in achieving high-quality final images and reducing uncertainty.

A prime example of this intricate relationship is the uneven adoption of single-sensor acquisition in challenging environments, like deserts (Somali and Taha, 2020). While some operators have embraced this method, others continue to collect data using traditional arrays. This divergence highlights the substantial processing challenges that originate from concerns over data quality (Bakulin et al., 2020; Ourabah, 2024). This study proposes a unified approach that integrates the Signal-Strength Estimate model (Meunier et al., 2011) with a data-driven signal-to-noise ratio (SNR) assessment (Bakulin et al., 2022b), aiming to close the loop between acquisition, processing, and quantitative interpretation for end users.

Signal-strength model

Considering that seismic image results from a combination of migration and stacking processes, Meunier (2011) popularized formula for estimating signal strength (SSE), which calculates the signal-to-noise ratio (SNR) of the final seismic image. The formula is given by:

$$SSE(f) = SS(f)\sqrt{SD\ NR\ RA}, \quad (1)$$

where *RA* is the are of the receiver array, *NR* the number of receivers per shot point, *SD* is the source density, *f* is a frequency, and *Ss* is the source strength. Incorporating *SD*NR* as trace density (TD) modifies the equation to

$$SSE(f) = Ss(f)\sqrt{TD\ RA}. \quad (2)$$

For vibroseis sources, source strength $Ss(f)$ is defined as

$$Ss(f) = Pf\ D\ N_v \sqrt{\frac{1}{Sr(f)}}\ , \quad (3)$$

where *Pf* is the peak force, *D* the drive level, N_v the number of vibrators in the source array, and *Sr(f)* the sweep rate *df/dt* (Meunier, 2011). *SSE* can be converted to theoretical *SNR* in decibels as $SNR_{dB}^{t} = 20\log_{10} SSE$.

Closing the loop

While the SSE model has been used in acquisition design, Bakulin and Silvestrov (2023) confirmed its accuracy with a realistic synthetic workflow, as shown in Figure 1. This method, improving on Regone et al. (2015), replaces processing with depth migration to remove human bias. They further refined the approach by introducing data-driven SNR analysis on imaged volumes for unbiased algorithmic ranking. Their findings show a strong correlation between SNR measured in six field geometries and the SSE equation, validating the square-root noise reduction model for handling coherent noise in challenging land seismic scenarios. This encourages applying a similar methodology to evaluate the shift from arrays to single sensors in 3D land seismic acquisition.

From arrays to single sensors

The SSE formula places arrays and single sensors on equal footing, allowing us to tackle this transition quantitatively. According to formula (2), substituting a geophone array with *N* elements requires an *N*-fold increase in trace density to achieve equivalent seismic image quality with single sensors. Most importantly, it states that this conclusion holds only *for identical source effort*. In a simple speak, the *N*-geophone array should be replaced by *N* single sensors or nodes for comparable results.

10.1190/image2024-4096021.1
© 2024 Society of Exploration Geophysicists and the American Association of Petroleum Geologists

Downloaded from http://pubs.geoscienceworld.org/segeab/proceedings-pdf/SEGEAB.43/1/228/7554982/image2024-4096021.1.pdf by University of Texas at Austin, Andrey Bakulin

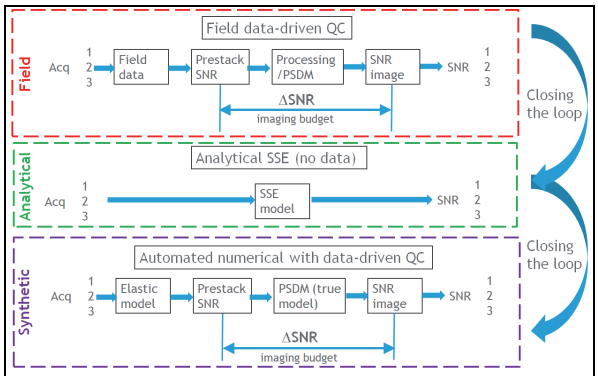

Figure 1: Three workflows aiding survey design, culminating in the SNR determination for seismic images across various acquisition geometries. By integrating these workflows with the analytical SSE approach (center), immediate understanding and analysis are achieved.

(transitioning from G4 to G5) leads to a SNR reduction of 3.5 dB for shallow and 1.2 dB for deep layers, aligning with the SSE equation's predicted 3.5 dB decrease. Despite a fourfold increase in trace density, the SSE (Signal-Strength Estimate) experiences a decrease, overshadowed by a ninefold reduction in array size, which negates the benefits of increased trace density. This drop in shallow SNR is clearly visible when comparing Figures 2b and 2a. The G6 single-sensor acquisition, with a trace density 16 times that of G4, surpasses the arrayed HCC data of G4, showing SNR increases of 2.3 and 1.3 dB for shallow and deep layers, respectively (as seen when comparing Figures 2b and 2c), nearly matching the SSE equation's anticipated 2.4 dB improvement. While not a perfect match, these results affirm the SSE equation's effectiveness even in complex, realistic synthetic scenarios.

The industry's enthusiasm for single-sensor recording (Baeten et al., 2000; Pecholcs, 2008; Mahgoub et al., 2015),

Name	**Short name**	**Shot spacing**	**Receiver Spacing**	**Trace density**	**SSE**	SNR^t_{dB} (shallow)	SNR^e_{dB} (shallow)	SNR^t_{dB} (deep)	SNR^e_{dB} (deep)
Narrow azimuth nodal HCC (3 × 3 geophone array, max crossline offset is ¼ of inline offset) (SD = 2, NR = 1.5, RA = 9)	G4	50 × 50 m	25 × 25 m	1	5.2	6.3 dB	6.4 dB	10.5 dB	11.6 dB
Nodal SS (intermediate) (SD=2, NR=6, RA=1)	G5	50x50m	25x25m	4	3.5	2.8 dB	2.9 dB	7 dB	10.4 dB
Nodal SS (dense) (SD=2, NR=24,RA=1)	G6	50x50m	12.5x12.5m	16	6.9	8.7 dB reference	8.7 dB reference	12.9 dB reference	12.9 dB reference

Table 1: Summary table outlines assessed geometries alongside their theoretical (SNR^t_{dB} from SSE model) and experimentally measured (SNR^e_{dB}) signal-to-noise ratios. Calibration between predicted and actual dB scales assumes $SNR^t_{dB} = SNR^e_{dB}$ for geometry G6. "HCC" refers to configurations with 9-geophone arrays designed for high-channel-count surveys, and "SS" signifies acquisitions employing single sensors. Identical source strength is assumed.

To numerically verify this, we implement a "synthetic" workflow (Figure 1), examining three geometries listed in Table 1, with their respective images and SNR volumes showcased in Figure 2. Denser than typical, narrow-azimuth Geometry G4 uses a standard 9-geophone array (Al Mesaabi, 2021, 2022) and limits cross-line offset to 1/4, enhancing sampling of noisy near offsets compared to the usual 100x100m setups. Transitioning to full-offset geometry single-sensor geometry G5, while keeping the same source-receiver grid, quadruples trace density but sacrifices the array. According to SSE equation 2, the interplay between trace density and receiver array size determines the SNR. Data from Table 1 and Figure 2 corroborate this finding. If aiming for single-sensor data with SSE comparable to array acquisition, trace density must be multiplied by nine (as per the nine-geophone arrays in our study). However, increasing trace density by only four times often viewed as the ultimate target, has elevated expectations far beyond what the SSE equation accounts for. Without introducing a quantitative counter to the SSE model, there's been an implication that single-sensor data might wield almost extraordinary powers to conquer noise, veering away from the basic square-root approach that forms the SSE's foundation.

A particularly insightful discussion that captures this sentiment comes from Ourabah (2024), who frames the debate around the question, "How many single-sensor nodes are needed to replace my array?" This study thoughtfully suggests that the answer isn't directly *N*, as the SSE equation might indicate, but often substantially less, perhaps even half. It also neglects to address source strength, suggesting it has no impact on the resulting image quality. The study states, "It's not uncommon to observe arrays of 12 or 6

10.1190/image2024-4096021.1
© 2024 Society of Exploration Geophysicists and the American Association of Petroleum Geologists

Downloaded from http://pubs.geoscienceworld.org/segeab/proceedings-pdf/SEGEAB.43/1/228/7554982/image2024-4096021.1.pdf by University of Texas at Austin, Andrey Bakulin

geophones being substituted by around 4 equally spaced single-sensor nodes, with the latter often delivering comparable or even enhanced results." However, it also warns that the ratio cannot be generalized blindly. In summary, this along with numerous other publications promoting single-sensor technology, challenges key aspects of the SSE framework, suggesting that trace density and spatial sampling are the sole determinants of the final seismic image's quality. Yet, these critiques fall short of offering an alternative quantitative model or a method for the optimal design of all survey parameters.

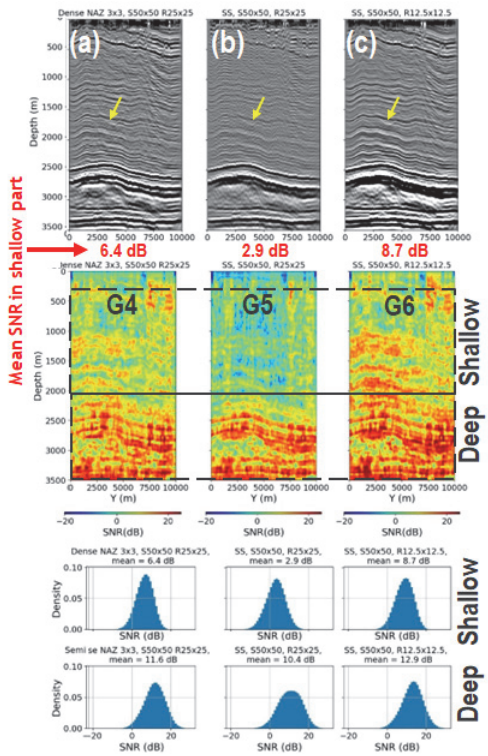

Figure 2: 3D PSDM cross-sections and SNR volumes for specific acquisition geometries: (a) Narrow-azimuthNodal HCC with 3x3 array, S50x50m, R25x25m, max crossline offset is ¼ inline offset; (b) SS with 3X trace density, S50x50m, R25x25m; and (c) Dense SS featuring 12X trace density, S50x50m, R12.5x12.5m. Following these, rows of histograms display SNR values within shallow (700-2000 m) and deeper (2000-3750 m) segments. "HCC" denotes high-channel-count configurations with 9-geophone arrays, and "SS" signifies single-sensor acquisitions.

We argue that dismissing the SSE model is premature and based more on hope than evidence. Recent work, utilizing controlled scenarios such as the SEAM Arid model and clear metrics like SNR, demonstrates the SSE model's continued relevance and accuracy, even without accounting for additional complexities like scattering speckle noise (Bakulin et al., 2022). We will further illustrate how the SSE model accurately reflects the critical role of source strength, a detail that alternative methods fail to capture.

The interplay of source strength and trace density

Current and legacy acquisition methods employ a source array with two vibrators. Nodal and blended acquisition techniques could gain productivity by utilizing a single vibe at the expense of halving the source strength (as per Equation 3). Rather than assuming a point source miraculously offsets this reduction in processing, a data-driven evaluation of field data is proposed. This involves applying the third "field" workflow shown in Figure 1 to examine the results of two concurrent 3D land acquisitions described by Tsingas et al. (2020). The first is a traditional survey employing a high-channel count 3D seismic, while the second utilizes a Distributed Source Array (DSA) approach with unconstrained blended shooting (refer to Table 2). This blended method permits the reduction of crossline distances for both shots and receivers from 125 meters to 75 meters without notably extending the acquisition timeline. However, this approach to blending does not use the two-vibrator arrays typical in production surveys, but rather single vibrators. If we embrace an alternative approach that

Acquisition type	Production	DSA
No. of receiver lines	48	73
No. of channels per line	480	441
No. of active channels	23,040	32,193
Shot point & receiver point distances (m)	25 x 25	25 x 25
Bin size (m)	12.5 x 12.5	12.5 x 12.5
Receiver line distance (m)	125	75
Shot line distance (m)	125	75
Nominal full fold	1808 (@ 6km offset)	5024 (@ 6km offset)
Trace density (per sq km)	11,000,000	32,000,000
Number of vibes per source array	2	1
Number of geophones per receiver array	9	9
Predicted SNR_{dB}^{t} (dB)	0 dB (reference)	-1.4
Measured SNR_{dB}^{e} (dB)	0 dB (reference)	-2
Acquisition type	Production	DSA blended

Table 2: Comparison of two field acquisitions from Tsingas et al. (2020): a traditional high-channel count survey and a Distributed Source Array (DSA) blended survey. Despite the DSA survey's threefold increase in trace density, the traditional survey reports higher SNR, aligning with both measurements and SSE predictions. This suggests that the benefits of increased trace density are overshadowed by the loss of the two-vibrator array, consistent with SSE formula expectations.

10.1190/image2024-4096021.1
© 2024 Society of Exploration Geophysicists and the American Association of Petroleum Geologists

Downloaded from http://pubs.geoscienceworld.org/segeab/proceedings-pdf/SEGEAB.43/1/228/7554982/image2024-4096021.1.pdf by University of Texas at Austin, Andrey Bakulin

moves away from the SSE model, focusing exclusively on trace density and channel sampling, the second survey demonstrates a threefold enhancement in trace density alongside a notable decrease in crossline sampling and should lead to better seismic image quality. Nevertheless, SNR measurements on the final stacks reveal that the blended survey's SNR is lower by -2 dB (Figure 3). Given that both datasets were processed using comparable workflows (Tsingas et al., 2020), this comparison should be equitable. This observation clearly cannot be explained by trace density and sampling alone.

In contrast, field results are readily explainable by SSE formula highlighting the importance of two key factors:

- Trace density increased by a factor of 2.9 (denser shot and receiver lines);
- The number of vibrators per source array dropped by a factor of two.

Equations (2)-(3) suggest that $SSE \sim N_v\sqrt{TD}$. The resulting SSE ratio between DSA and production is 0.85, translating into an SNR difference of -1.4 dB (Table 2). As a result, the predicted (-1.4 dB) and measured (-2 dB) average SNR differences are comparable. Further analysis indicates that to match the SNR ratio of the production survey, the DSA survey must see a 4-fold increase in trace density (compared to the initial 2.9 implemented). To exceed the SNR ratios of the production survey, a more significant increase in trace density is required.

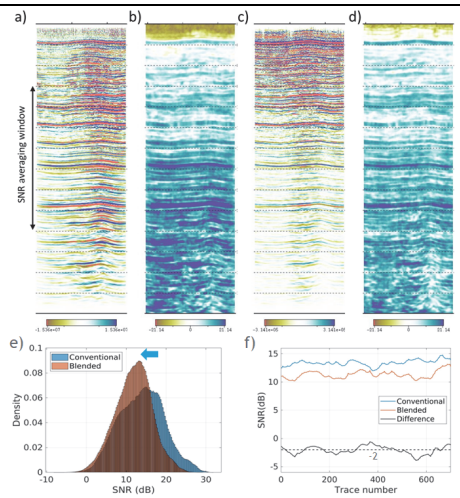

Figure 3: Figure 2 displays seismic images and SNR for a high-channel count production acquisition (a,b) and a blended DSA acquisition (c,d), with histograms in (e) illustrating SNR distribution in a specified time window. SNR curves in (f) average these values, showing the DSA acquisition reduces SNR by approximately -2dB, a discrepancy visible upon visual inspection. This measured -2dB difference aligns closely with the -1.4 dB predicted by the SSE equation, affirming its predictive accuracy.

Discussion

Our results underscore the SSE's robustness and comprehensive nature, supported by solid, data-driven SNR analysis. Visual comparisons often lead to endless debate without clear resolution. A practical approach favors established metrics for evaluating image quality, with SNR being a critical measure for interpreters and geologists, unlike trace density which provides an incomplete picture.

While machine learning and nonlinear methods might surpass the SSE model's square-root law in noise suppression and imaging, solid proof is still pending. The low SNR of single-sensor data (Cordery, 2020; Bakulin et al., 2022b; Ourabah, 2024) complicates finding methods that beat traditional stacking. Similarly, optimal stacking techniques have had limited success over conventional stacking, mainly because accurately setting optimal weights in low SNR conditions is challenging (White, 1977).

While SSE may miss some finer details as a basic model, no alternative yet offers comparable guidance for survey design. The model's reliability is confirmed through both field and synthetic workflows. We propose using the SSE model systematically for outcome comparison and model refinement, leveraging discrepancies to improve the SSE approach.

Conclusions

Pursuing superior seismic survey designs is a common objective across the industry, yet navigating toward this goal without a quantitative acquisition model is like sailing without a compass. Our findings affirm that the established SSE model, despite its imperfections and potential need for adjustments, stands validated against the rigors of transparent, data-driven metrics, moving beyond the realm of subjective expert judgments. Presently, there exists no alternative quantitative framework that encapsulates the combined impact of crucial acquisition parameters as comprehensively as the SSE model does. We propose the adoption of straightforward, universal metrics such as data-driven SNR statistics to begin evaluating the efficacy of both innovative and traditional acquisition methods. By sharing these metrics within the geophysical community, we can quantitatively assess the extent to which seismic acquisition techniques enhance the image quality for end-users.

Extending a similar methodology to prestack data and processing will allow us to define the SNR thresholds at which our algorithms remain effective. Furthermore, incorporating the consideration of speckle scattering noise becomes essential to achieving success with prestack data inversion, showcasing another critical aspect that must be captured to fully realize the potential of seismic acquisition advancements.

10.1190/image2024-4096021.1
© 2024 Society of Exploration Geophysicists and the American Association of Petroleum Geologists

Downloaded from http://pubs.geoscienceworld.org/segeab/proceedings-pdf/SEGEAB.43/1/228/7554982/image2024-4096021.1.pdf by University of Texas at Austin, Andrey Bakulin

REFERENCES

Al Mesaabi, S. A., G. Camboi, J. Cowell, D. Arnold, M. F. Boukhanfra, S. H. Al Karbi, and M. Mahgoub, 2022, The world's largest contiguous onshore and offshore 3D seismic survey is getting even larger: Abu Dhabi International Petroleum Exhibition & Conference, SPE, https://doi.org/https://doi.org/10.2118/211687-MS

Al Mesaabi, S. A., G. Cambois, J. Cowell, D. Arnold, M. F. Boukhanfra, S. H. Al Karbi, M. Mahgoub, and K. Obaid 2021, Lessons learned from the world's largest continuous onshore and offshore 3D seismic survey: Abu Dhabi International Petroleum Exhibition & Conference, SPE, https://doi.org/https://doi.org/10.2118/208009-MS.

Baeten, G. J. M., V. Belougne, L. Combee, E. Kragh, A. Laake, J. Martin, J. Orban, A. Özbek, and P. L. Vermeer, 2000, Acquisition and processing of point receiver measurements in land seismic: 70th Annual International Meeting, SEG, Expanded Abstracts, 41–44, https://doi.org/https://doi.org/10.1190/1.1816083.

Bakulin, A., D. Neklyudov, and I. Silvestrov, 2022a, Multiplicative seismic noise caused by small-scale near-surface scattering and its transformation during stacking: Geophysics, **87**, no. 5, V419–V435, https://doi.org/https://doi.org/10.1190/geo2021-0830.1.

Bakulin, A., and I. Silvestrov, 2023, Quantitative evaluation of 3D land acquisition geometries with arrays and single sensors: Closing the loop between acquisition and processing: The Leading Edge, **42**, 310–320, https://doi.org/https://doi.org/10.1190/tle42050310.1.

Bakulin, A., I. Silvestrov, and M. Protasov, 2022b, Signal-to-noise ratio computation for challenging land single-sensor seismic data: Geophysical Prospecting, **70**, 629–638.

Bakulin, A., S. Silvestrov, M. Dmitriev, N. Neklyudov, M. Protasov, K. Gadylshin, and V. Dolgov, 2020, Nonlinear beamforming for enhancement of 3D prestack land seismic data: Geophysics, **85**, no. 3, V283–V296, https://doi.org/https://doi.org/10.1190/geo2019-0341.1

Cordery, S., 2020, An effective data processing workflow for broadband single-sensor single-source land seismic data: The Leading Edge, **39**, 401–410, https://doi.org/https://doi.org/10.1190/tle39060401.1

Mahgoub, M., Y. Seo, A. Dhafra, G. Busanello, C. Roig, and A. Glushchenko, 2015, Paradigm shift from seismic array to S4 in acquisition and processing; Case study of onshore 3D seismic: Abu Dhabi International Petroleum Exhibition and Conference, SPE, https://doi.org/https://doi.org/10.2118/177781-MS.

Meunier, J., 2011, Seismic acquisition from yesterday to tomorrow: SEG and EAGE, 2011 Distinguished Instructor Course, Distinguished Instructor Series, No. 14, https://doi.org/https://doi.org/10.1190/1.9781560802853.

Monk, D., 2020, Survey design and seismic acquisition for land, marine, and in-between in light of new technology and techniques: SEG, https://doi.org/https://doi.org/10.1190/1.9781560803713.

Ourabah, A., 2024, Revisiting the single sensor vs array debate in the light of new nodal system technology: First Break, **42**, 71–77, https://doi.org/https://doi.org/10.3997/1365-2397.fb2024006.

Pecholcs, P. I., 2008, A history of seismic acquisition design in Saudi Arabia-lessons learned: EAGE Vibroseis Workshop-Vibroseis Acquisition and Processing Half Century Later, New Developments in Data Quality and Productivity, https://doi.org/https://doi.org/10.3997/2214-4609.20147523.

Regone, C., M. Fry, and J. Etgen, 2015, Dense sources vs. dense receivers in the presence of coherent noise: A land modeling study: 85th Annual International Meeting, SEG, Expanded Abstracts, 12–16, https://doi.org/https://doi.org/10.1190/segam2015-5833924.1.

Somali, F., and Y. C. El-Taha, 2020, Geophysicists meet in Muscat to discuss advancements in land geophysical acquisition technologies: The Leading Edge, **39**, 434–435, https://doi.org/https://doi.org/10.1190/tle39060434.1.

Tsingas, C., M. S. Almubarak, W. Jeong, A. Al Shuhail, and Z. Trzesniowski, 2020, 3D distributed and dispersed source array acquisition and data processing: The Leading Edge, **39**, 392–400, https://doi.org/https://doi.org/10.1190/tle39060392.1.

White, R. E., 1977, The performance of optimum stacking filters in suppressing uncorrelated noise: Geophysical Prospecting, **25,** 165–178, https://doi.org/https://doi.org/10.1111/j.1365-2478.1977.tb01159.x.

© 2024 Society of Exploration Geophysicists and the American Association of Petroleum Geologists

Downloaded from http://pubs.geoscienceworld.org/segeab/proceedings-pdf/SEGEAB.43/1/228/7554982/image2024-4096021.1.pdf by University of Texas at Austin, Andrey Bakulin